KINETIC FAST IGNITION FUSION

Colin Bruce Jack

ColinBJ@gmail.com

ABSTRACT

This is the first fusion method provably viable at utility scale. Energy input is by charged pellets fired at ultraspeed from modified particle accelerators, a technique routinely used to test spacecraft meteor shields, and first proposed as a fusion driver 50 years ago. A key enabling technology, now available, is the ability to track and steer individual pellets in flight, permitting very precise delivery independent of distance from accelerator to target. A train of pellets fired at successively increasing speed catch up together over a long flightpath to arrive as a unit: an accelerator of modest power can deliver an intense input.

For an efficient fast ignition strategy, medium-speed pellets impact and heat a hohlraum, causing 3-D compression of a hemispherical fuel capsule within. Smaller faster pellets fired from a parallel accelerator converge into a dense bullet, which strikes the compressed fuel to ignite it.

Technical risk is negligible because:
- Fuel compression required is less than already achieved in NIF.
- Subsequent ignition is so rapid that there is no chance for instabilities to disrupt it by fuel redistribution or mixing.
- All materials and components required have been successfully manufactured.

The system can burn deuterium-tritium fuel closely and completely surrounded by lithium, for a closed fuel cycle with no radioactivity issues. Capital cost will be modest: it may even be possible to modify existing coal-fired plant for fusion.

Key features are claimed in patents currently in the national phase worldwide.

1. INTRODUCTION

The simplest possible method of igniting fusion, proposed long before powerful lasers existed, is by firing a bullet into a deuterium-tritium target. Winterberg[1] pointed out 50 years ago that while accelerating a monolithic bullet to the necessary speed is impractical, charged pellets could be fired from a modified particle accelerator to converge into the bullet required. Charged pellets are now routinely fired from modified particle accelerators at speed ~100 km/sec to test spacecraft meteor shields.

Proceeding to fusion is not trivially easy because it is now recognized that[2]:

- Some 3-D precompression of the fuel is necessary, compression by impact alone is insufficient
- The impact speed necessary for ignition is high, 5,000 km/sec

However enabling technology now exists for the following implementation:

- Medium-speed pellets impact and heat a hohlraum, causing modest NIF-style 3-D compression of a hemispherical fuel capsule within it
- Smaller faster pellets provide a relatively small additional energy input to ignite the fuel
- AC accelerators powered by thumbnail-size RF MOSFETs deliver both pellet types
- ADC sampling at GHz rates permits individual pellet course measurement and correction, for micron-precise delivery at any range
- Active course correction, unlike focusing by quadrupoles, is compatible with non-spherical pellets such as long thin fibers, which can hold a much better charge/mass ratio than microspheres

Technical risk is minimal because:

- The initial fuel density needed is less than that already achieved in NIF
- Ignition energy is delivered so fast there is no opportunity for Rayleigh-Taylor or other instabilities to disrupt ignition by fuel motion or mixing
- Sufficient energy can be delivered at sufficient rate that it follows from basic momentum and energy conservation that the ignition threshold will be surpassed, whether or not modelling such as [2] proves to be accurate
- With ignition temperature ≥12 keV, good burn from an isochoric hot spot is obtained even with non-spherical or irregular fuel shape: use of a hemispherical fuel capsule whose implosion speed may vary slightly with polar angle is well tolerated

- All materials and components required have been successfully manufactured: most are commercially available
- Continuous high performance operation of a pellet accelerator has been demonstrated even using heavily contaminated source material, electrostatic lensing ensuring that material not having exactly the correct charge/mass ratio does not enter the accelerator[3]

System cost is modest because:
- Pellets fired at successively increasing speed catch up together over a long flightpath: accelerators of modest power, firing over a relatively long period, deliver brief intense inputs of energy
- The high charge/mass ratio possible with fibers allows accelerator length to be kept reasonable
- Radioactivity issues will be negligible because the fuel burn can be closely and completely surrounded by liquid lithium, productively capturing all neutrons produced
- It may be feasible to retrofit existing coal-fired plant for fusion

As shown in section 2, capital cost of a new 1 GW fusion power station will be comparable to a coal-fired plant, ~$3 billion. Existing coal-fired plant can be modified for fusion for a fraction of that price.

As shown in section 3, a particular attraction for private development is that the key capability, accelerating a macroscopic fiber to fusion speed and controlling its trajectory, can be demonstrated quickly at modest cost. From that point, proceeding to power generation is merely a matter of scaling.

2. COSTED EXAMPLE : 1 GW POWER STATION

2.1 Introduction

Energy must be delivered to perform two separate tasks. For fuel precompression, a hohlraum is heated to 300 eV by 4 MJ of kinetic energy delivered at relatively low speed ~1,000 km/s. For ignition, a small sub-volume of the compressed fuel is heated to ~12 keV by 43 kJ of kinetic energy delivered at higher speed ~6,000 km/s.

The hohlraum-heating pellets are 40× the diameter of the ignition pellets, but travel 6× slower with specific kinetic energy 36× lower. Because the charge/mass ratio that a pellet can be given is inversely proportional to its diameter, parallel accelerators of similar length, housed in the same building, can launch both sets.

Two effects are used for convergence so that initially long trains of pellets (several hundred metres in length) deliver their energy at the same place and time.

- Longitudinal convergence: pellet speed within a train varies, lower for the first pellets fired to higher for the last, so the entire train closes up together as it travels.
- Micro scale convergence. Each pellet is a charged fiber which is initially stretched taut by self-repulsion. On discharge, it contracts into a tight bundle, just as a stretched elastic band contracts when released.

2.2 Ignition requirement

The ignition energy needed is a function of fuel density. 3D simulation of a specific impact case[2] has found that for fuel density 200 g/cc, impact of a cylindrical gold bullet of length and diameter 40 microns (density 19.3 g/cc, mass 0.97 µg) at 5,000 km/s achieves ignition. The gold bullet turns to plasma and widens to diameter 45 microns during impact. Nominal energy delivery parameters (if the bullet was infinitely compressible and struck an immovable object) are shown in Table 1 column 4: column 5 shows these parameters rescaled as required for 100 g/cc fuel as described in Appendix 2. We can match these values by delivering pellets of mass 2.4 µg travelling at average speed 6,000 km/s.

Table 1   **Ignition energy delivery**

Bullet		units	From [2]	Scaled for 100 g/cc fuel	Provided
Kinetic energy	**E**	kJ	12	43	43
Energy rate	**W**	PW	1.5	3	> 10
Energy intensity	**I**	PW/mm²	950	490	> 10^3
Diameter at impact	**D**	μm	45	89	89
Areal energy	**S**	J/μm²	7.5	7.0	7.0

Looking ahead to the cost estimates in section 2.12, note that it would be possible to deliver many times more energy than column 6 if necessary, exceeding all thresholds by a high multiple.

We deliver pellets comprising fibers of S-2 glass of normal solid density 2.46 g/cc, travelling at 5,400 – 6,600 km/s. A simple simulation program (available free on request) shows that if the initial length/width ratio at solidity of the cylinder formed by the converging pellets ≥ 5, then the density ratio achieved when the length of the compressing cylinder becomes equal to its diameter is solely a function of the convergence speed, the relative speed of the first and last pellets. With convergence speed 1,200 km/s this ratio is 4, to density ~10 g/cc. Subsequently the cylinder length rapidly becomes shorter and the density many times greater, but the diameter has time to grow only slightly as maximum density is achieved.

The pellets initially converge into a solid cylinder of diameter 50 microns and length 500 microns at S-2 glass normal density, through length = diameter = 75 microns at density 7.2 g/cc, to ultimate diameter 89 microns with length a few microns and very high bullet density. This gives the figures shown in the final column of Table 1.

Note that we provide average fuel density ~400 g/cc, as shown in section 2.3 below, at which ignition energy would theoretically be lower. However the ignition bullet energy cannot necessarily reach the densest part of the fuel: [2] unrealistically assumes a sharp boundary between zero and maximum fuel density. Spherical compression simulations show a gradient of fuel density doubling every ~2–8 μm[4, p57, Figure 3.8b][5, p8, last Figure], a similarly sharp gradient is achievable with a hemispherical fuel capsule[6, Figure 7]. The final areal mass of our bullet is .039 g/cm², equivalent to a 3.9 μm layer of 100 g/cc fuel. The bullet will heat fuel one-half radius

= 22 μm ahead of its nominal front effectively. When the bullet has struck fuel equal to its own mass, the density at this leading point will be ≥ 100 g/cc, even on a very pessimistic density gradient assumption of 10 μm doubling distance.

Radiated energy travels ahead of the bullet into the fuel at the speed of light, 50× the bullet speed, and ignition occurs well ahead of the interface between bullet material and fuel. The growth rate of Rayleigh-Taylor instabilities tends to zero when there is a large density ratio between the colliding substances, as is the case when the bullet first meets thinner plasma (because the acceleration of the interface is low, and growth rate of RT instabilities is ~√ of this acceleration[4, p239-240]). Thus there is no opportunity during the collision for the fuel to become sufficiently poisoned by mixing to prevent ignition.

Note that the fuel density doubling distance is small compared to the linear dimensions both of our bullet and that in [2], and our bullet arrives precompressed to a much shorter length/width ratio than that of [2]. Thus the proportion of energy lost during the early part of the collision, before the desired density and temperature are attained, will be less than [2] despite the non-sharp fuel boundary.

2.3 Fuel compression energy

A fairly large output of 400 MJ thermal fusion energy per detonation is chosen as convenient. Induced fission in the surrounding Li waterfall will add 100 MJ[4, p45] for total 500 MJ.

Burn fraction from an isochoric hot spot is calculated differently from isobaric central ignition as in NIF: a burning wave propagates from the hot spot, and burn fraction does not depend primarily on ρR containment, but on the quantity of inward kinetic energy input for compression. The relevant formulae are (from [4, p413], equation 12.6 illustrated in Figure 12.3):

G = 1.8 × 10⁴ × E⁰·⁴ / α¹·²   **[Eqn. 1]**

G = 4.2 × 10³ × M⁰·³ / α⁰·⁸⁷   **[Eqn. 2]**

where **G** is energy gain ratio, **E** is fuel kinetic energy in MJ, **M** is fuel mass in mg, and isentrope parameter **α** = 1.5.

From Eqn. 1, an input of **100 kJ** results in gain G of 4,400, hence fusion output of 440 MJ, a 10% margin over what is required. From Eqn. 2 fuel mass is 3 mg. The implied fuel implosion speed for 100 kJ KE is 260 km/s.

Full burn of DT yields 337 MJ/mg[4, p46], so the implied burn fraction is 40%, reasonable for fast ignition.

Fuel density

The most reliable way to calculate the fuel density we will achieve is to scale from a known NIF result. Fuel compression is quasi-isentropic. The energy required thus follows the adiabatic equation $E \sim ((V_1/V_2)^{(\gamma-1)} -1)$ where V_1 and V_2 are the initial and final volumes and γ is the ratio of specific heats. For plasma $\gamma = 5/3$, so for large compression ratios:

$$E \sim (V_1/V_2)^{(2/3)} \qquad \textbf{[Eqn. 3]}$$

NIF performance

The NIF can compress 0.157 mg DT fuel with fuel implosion speed 350 km/s, fuel kinetic energy 9.6 kJ, achieving density ~600 g/cc[7]. A quarter of that kinetic energy goes to compress the central gas volume, without this the implosion speed needed would reduce to 300 km/s.

The rocket equation tells us that the mass ratio (the ratio of payload mass to initial mass) required is $e^{v/w}$ where w = rocket exhaust speed and v = final payload speed. In [7] mass ratio 12.5 gives final payload speed 350 km/s, implying exhaust speed ~140 km/s, from hohlraum temperature ~300 eV. The ideal minimum work done at the evaporating surface is 10 kJ/mg propellant, 27 kJ. The X-ray energy absorbed by the propellant is not measured directly, but is estimated ~8× this, ~200 kJ.

Our performance

We need implosion speed 260 km/s. Mass ratio using the same exhaust speed as NIF, 140 km/s, reduces to 6.4, requiring 16 mg plastic to propel our 3 mg DT fuel. Ideal minimum work on the evaporating surface 10 kJ/mg = 160 kJ, 5.9× greater than NIF.

Note that compared to NIF less energy is wasted as residual kinetic energy of the propellant: as with any rocket, lower ratio of payload speed to exhaust speed gives better efficiency.

Our fuel has ~0.75 the specific kinetic energy which NIF would require to reach its 600 g/cc density if no work was done compressing the central gas: we will achieve average fuel density ~0.65 that of NIF, ~400 g/cc.

2.4 Pellets

As shown in Appendix 1, the maximum charge/mass ratio that a macroscopic pellet can be given without breaking up is a function of its tensile strength, shape and size. Metal-coated S-2 glass fibers are ideal:

- S-2 glass has excellent strength, increasing from 5 GPa in a room environment to 8.3–11.6 GPa if cooled to cryogenic temperature[8].

- In contrast to carbon fibers, glass fibers can be made in a wide range of diameters: full strength at diameters down to 50 nm can be achieved simply by two-stage drawing[9].

- Glass fibers have useful radial as well as longitudinal strength.

- A vacuum-deposited aluminum coating allows charge to equilibrate on the fiber surface without damaging it. If this coating is thicker or supplemented with a denser metal at the points where the fiber will be cut, then individual fibers can be ballasted to have a constant charge/mass ratio along their length, despite the higher charge near the endpoints.

Table 2 : Pellet Characteristics

Type	IG	HH
Diameter	0.25 μm	10 μm
Length	2.0 mm	4.16 mm
Mass	0.24 ng	800 ng
Charge	170 pC	14 nC
Charge/Mass	700 C/kg	17.5 C/kg
Mean speed	6,000 km/s	1,000 km/s
Number	10,000	10,000
Total mass	2.4 μg	8 mg
Total KE	43 kJ	4 MJ
Max surface gradient	~2 V/Å	~2 V/Å

Pellet parameters are shown in Table 2. Usefully, the accelerating voltage required is identical for both types of pellet. The ignition pellets have 1/40 the diameter of the ignition pellets, so can carry a charge/mass ratio 40× greater. The fastest HH pellets are fired at 1,100 km/s, the fastest IG pellets at 6,600 km/s. The drive voltage needed is **34.5 GV** for the HH accelerator and **31 GV** for the IG accelerator.

2.5 Accelerators

Maximum pellet speed is ~2% lightspeed. This has two beneficial consequences for the accelerator design, as compared to a fundamental particle accelerator:

- Drive frequency can be two orders of magnitude lower. Cheap MOSFET chips rather than klystrons can provide the power.
- Electrodes can be spaced closer together. While dielectric strength is conventionally expressed in volts per metre, breakdown voltage of an inter-electrode gap (whether occupied by solid insulator or vacuum) is actually proportional to the square root of the gap width. A higher drive voltage per metre results if closely spaced electrodes can be used.

Current state of the art for particle accelerators[10] is 38 MV/m. However that applies to a conducting wall accelerator whose electrodes act as RF resonant cavities. For our much lower pellet speed and frequency, electrodes separated by insulators are used. This arrangement is more similar to a gun such as [11], which currently achieves 190 MV/m, and 127 MV/m even before advanced electrode conditioning. This value is for a pulse of duration 0.7 µs at effective electrode separation 2.4 cm. A technical note to an industry standard electrical design program[12] gives a scaling law $E_{max} \sim 1/V.\tau^{0.34}$, where **V** is the voltage between adjacent electrodes and τ is pulse length. This can be rewritten as:
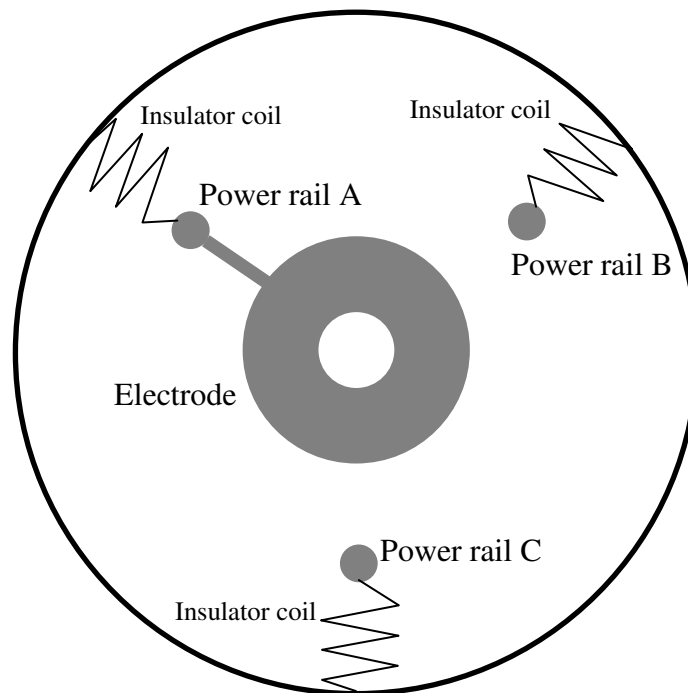
$$E \sim L^{-0.5}.\tau^{-0.17} \qquad \textbf{[Eqn. 4]}$$

where **L** is the distance between electrodes. We are using electrode separation 1 cm, and longest pulse length for any electrode is 1 ms, at a point one-third of the way along the HH accelerator: the 127 MV/m value from [11] extrapolates to 61 MV/m. Allowing for geometrical factors such as finite electrode thickness, **40 MV/m** is a conservative assumption: 863 m accelerator length gives the **34.5 GV** drive voltage required. This is rounded up to **900 m** to allow for course correction stations as described in section 2.8 below. The parallel IG accelerator could be slightly shorter, due to the slightly lower voltage and significantly shorter pulse length required.

To avoid vibration, each fiber should perceive a field which is spatially uniform and/or does not vary with time. This can be achieved if 3 phases are used (the equivalent trick with 3 phases is well known for electromagnetic coilguns).

Because pellet speed is small compared to lightspeed and the accelerator electrodes do not act as resonant cavities, an open design as shown in cross-section in Figure 1 can be used. The insulating mounts are ceramic coils: dielectric breakdown over the surface of the insulator is not a limiting factor. Power rails for 3-phase power are provided alongside the electrodes: the example shown is connected to rail A. Note that at any given instant, all electrodes in an accelerator tube are operating at the same frequency.
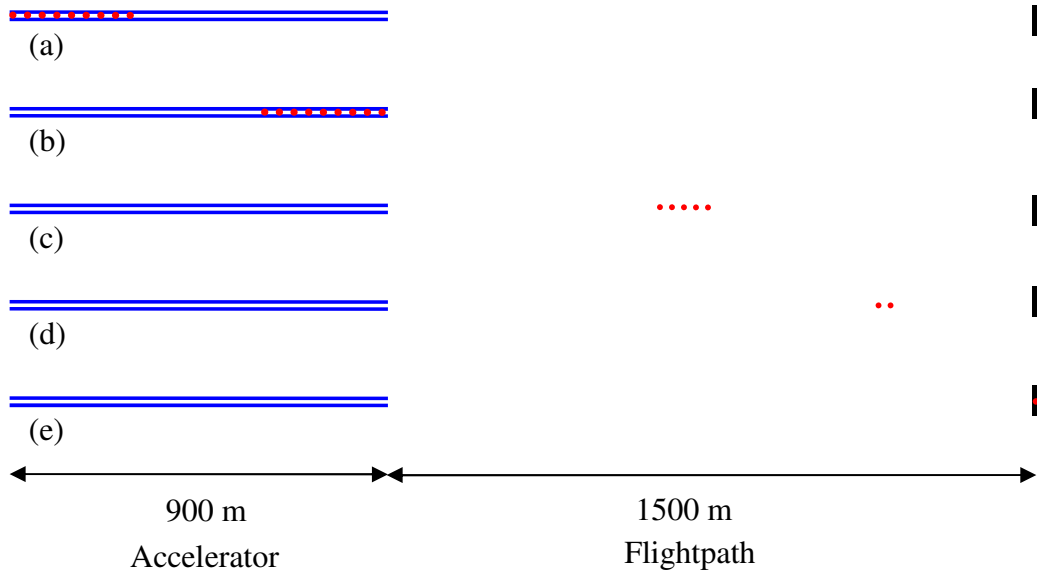
Figure 1   Accelerator tube cross-section

2.6 Operational sequence

The operational sequence is illustrated in Figure 2. It is similar for both accelerators.

Figure 2   Accelerator operation

900 m
Accelerator

1500 m
Flightpath

HH accelerator

1. This accelerator is loaded by inserting glass fibers through 10,000 holes set at 30 mm intervals along the first 300 m of its length. Continuous fiber is fed from coils: upon charging and chopping by laser to the required length, self-repulsion stretches each fiber taut.

2. The pellet train is accelerated at 6.5 x 10^8 m/s². Pellet separation remains constant: all electrodes are driven at the same frequency, which increases continuously. The first pellet emerges after 600m of acceleration, at 900 km/s. The last pellet emerges after 900m of acceleration, at 1,100 km/s. The peak drive frequency is 36.6 MHz.

The HH pellets arrive at the target as a hollow cylindrical cloud 15 mm in diameter × a few cm in length after travelling 1500 m from their accelerator exit.

IG accelerator

The IG pellets are launched from their parallel accelerator just over 1 ms after the HH pellets, catching up en route to arrive at the target just nanoseconds later, as the

target reaches maximum density. The accelerator operational sequence is almost identical, but for speed 6× higher:

1. The pellet train is accelerated at 2.34 x 10^10 m/s².

2. The first pellet emerges at 5,400 km/s, the last at 6,600 km/s.

3. The peak drive frequency is 220 MHz.

The IG pellets converge into a compact bullet as described in section 2.2 after travelling 1500 m from their accelerator exit.

2.7 RF power supply

A suitable unit is the IXZ2210N50L RF power MOSFET, which can produce 550W CW at 175 MHz[13]. Operating voltage is 150V, so the output passes through one or more stages of small open-core transformers en route to the electrodes: 20% power loss downstream of the MOSFETs is assumed. Maximum instantaneous output is limited by the unit's reactance, and varies with frequency[13, Mag S21 column in final table] approximately as $f^{-1.5}$.

Maximum output per pulse train is moreover limited by resistive heating to ~6 J per MOSFET for ~1 ms pulse train. ([13]Safe Operating Area graph, multiply by 1.83 for IXZ2210N50L relative to IXZ210N50L.)

At the fast end of the IG tube, the fast end electrode frequency peaks at 220 MHz as the final pellet exits. However maximum power is required just before the first pellet exits. 2.4 μg of pellets are being accelerated at 2.34 $\times 10^{10}$ m/s², force 56 N at 5.4×10^6 m/s, work rate 300 MW. At this moment the frequency is 180 MHz, available output per MOSFET 527 W. Allowing for 20% downstream loss **570,000 units** are needed. Total energy supplied is 52 kJ, < 0.1 J/unit, so resistive heating is not a constraint.

For the HH tube, maximum power is likewise required just before the first pellet exits: 8 mg of pellets are being accelerated at 6.5×10^8 m/s², force 5.2 kN at 0.9×10^6 m/s, work rate 4.7 GW. At this moment the frequency is 30 MHz, available output per MOSFET 7.75 kW, allowing for 20% downstream loss this implies 758,000 units. However energy supplied is 4 MJ net, allowing for losses 5 MJ must be output, so this increases to **833,000 units** to stay within the 6 J/unit resistive heating limit.

MOSFET cost is $70/unit[14], so the total **1.4 million units** will cost $100 million.

2.8 Focusing

As with a fundamental particle accelerator, mutual repulsion will tend to push pellets away from the beamline. Fundamental particle accelerators use electromagnet quadrupole focusing: at pellet speed low compared to light, cheaper electrostatic rather then electromagnetic quadrupoles could in principle be used. However quadrupole focusing is not compatible with long fibers, which would tend to resist focusing in the direction parallel to the fiber axis, and also to be rotated by each quadrupole, acquiring unwanted angular momentum. Fortunately there is a better alternative for macroscopic objects: active guidance.

For macroscopic pellets, nearest neighbor effects dominate defocusing: the most challenging pattern is alternating pellets deflecting in opposite direction in a zigzag pattern. The lateral field needed for correction is small compared to the steering field which can be exerted even at large zigzag amplitudes. A more critical parameter is the time constant for a pellet's deviation from the beamline to double due to lateral acceleration. Within the accelerators, at full charge with inter-pellet separation 3 cm, this time constant is ~110 µs for IG pellets and ~60 µs for HH pellets. Acceleration duration is up to 0.3 ms for IG pellets and 2 ms for HH pellets, so within-accelerator course correction is needed at ~5 waypoints for IG pellets and ~50 waypoints for HH pellets. The associated position measurement stations are set within metal tubes in gaps in the accelerator, which act as Faraday cages to screen out external fields (alternatively, measurement is performed optically).

The easiest way to measure pellet position (and optionally orientation) is by ADCs connected to loops immediately adjacent to the beamline. 14-bit ADCs capable of suitable sampling rate are commercially available at ~$50/Msps (million samples per second)[15]. Subsequent course adjustment (and optionally, also spin rate/orientation adjustment) is performed by rapidly switched electrodes adjacent to the beamline.

As the pellets subsequently close up together in ballistic flight, the defocusing time constant would reduce: to avoid this they are discharged in stages, the first just after they leave the accelerator, the last just after the final course correction.

IG and HH pellets follow near-parallel lines which meet at the hohlraum. Note that the HH pellets travel ahead of the IG ones, so there is no problem of interaction between the two types. Arrival point of each HH pellet can be selected independently at its final course correction, so the heating pulse caused by their impact on the hohlraum foil can be tailored in software to the spatial and temporal configuration found optimal.

2.9 Discharge

Discharge after the pellets leave the accelerator is done in stages, so that the pellets retain sufficient charge to be steerable without inter-pellet repulsion becoming excessive as linear convergence occurs. Discharge is by spraying with electrons.

Discharging the fibers by dropping a matching charge of electrons on them from effective infinity would release energy ½QV, where V is the initial surface potential, sufficient to melt them. Note that at the voltages involved, the penetration depth of the electrons considered as beta rays is much greater than the fiber diameters, so heating is relatively uniform throughout the volume of the fiber.

There are two solutions to this problem.

- Fibers oriented normal to the beamline and parallel to one another can pass between electrodes forming roughened walls spaced much less than one fiber length apart. Electrons pulled from the walls onto a fiber arrive with far less energy than they would dropped from 'infinity'.

- Fibers can be coated with metal whose evaporation point is lower than the softening point of S-2 glass. Field evaporation will ensure positively charged ions escape from this surface at relatively modest temperature. Far fewer electrons are needed to cause the necessary heating than would be required to neutralise the whole charge.

The second solution is preferred.

(Note that because ballistic electrons in vacuo donate their kinetic energy to the target not the source, corresponding heating does not occur on initial pellet charging.)

At final discharge, tension causes the fibers to contract with the ends approaching the centre at several hundred m/s. Nominally, each fiber should collapse into a sphere of diameter ~7 μm for IG fibers, ~100 μm for HH fibers. This assumes that there is no fiber rotation or vibration: however any such motion will be small compared to the inward speed, and much larger regions are acceptable, up to ~50 μm diameter for IG fibers and ~1 mm diameter for HH fibers.
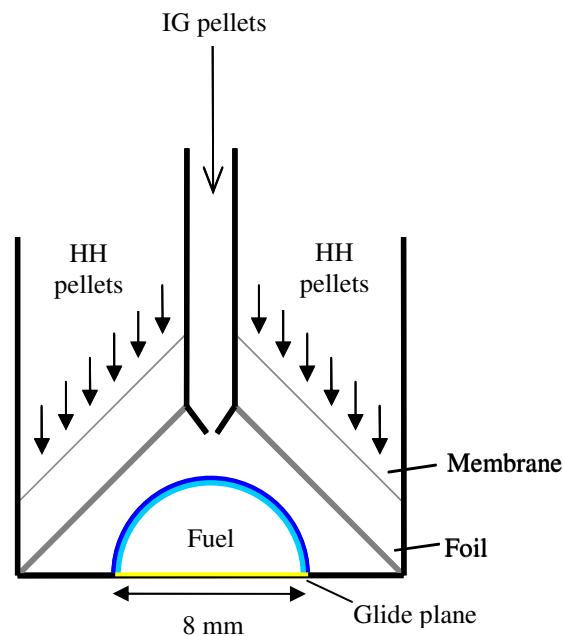
2.10 Fuel capsule and hohlraum

A fuel capsule in the form of a hollow hemisphere 8 mm in diameter contains 13 mm^3 DT ice within an outer shell of CH plastic. This hemisphere rests on a glide plate of high-z material within a hohlraum as shown in Figure 3. The initial hemisphere

shape will not collapse to a perfect sphere, nor will ignition be at its precise centre of mass, but these factors are known to have little effect on fast ignition.

The hohlraum is heated by pellets entering in the direction of the short arrows. The first pellets strike a thin 1 μm membrane, releasing enough energy to completely vaporize both the membrane and the pellets already within the hohlraum. The incoming HH pellets have KE of several hundred eV: less than 1 eV is sufficient to vaporize solid matter. The evaporated pellet material proceeds to strike a carbon foil of thickness 0.1 mm, mass 32 mg. The foil also turns to plasma, heated through by penetrating X-rays and electrons. The hohlraum temperature is now high enough that all subsequent pellets are also vaporized well before impact.

The pellets, of total mass 8 mg and average speed 1,000 km/s, supply 4 MJ kinetic energy. Because the foil mass is several times the pellet mass, and the duration of the collision process is only a few tens of ns with most of pellet mass striking toward the end of this period, from conservation of momentum the collision plasma formed from the foil and pellet mass moves only ~2 mm during the entire period, reaching a final speed of 200 km/sec = 200 μm/ns and remaining well clear of the receding wall of the fuel capsule.

Figure 3   Hohlraum

Some physicists have difficulty correctly visualizing the collision, for example wrongly thinking that 'shattering' of the foil could disrupt the process, or that pellet fragments might somehow pass through the foil or the plasma formed from it. See

for a technical note containing FAQs, contact **ColinBJ@gmail.com** if you have further queries.

Note that material which ablates from the outer surface of the fuel capsule to compress it forms an exhaust gas which protects the imploding fuel from any possible interference by fast electrons or ions emitted from the collision plasma.

At its final temperature 300 eV the collision plasma contains 1.01 MJ heat energy (electron and ion temperatures assumed equal, average particle mass 1.71 amu). From conservation of momentum it is moving at 200 km/s, so it also has 800 kJ kinetic energy. The remaining 2.19 MJ of the original kinetic energy is radiated as X-rays. It is radiated equally to both sides of the collision plasma, and not all of the inward-radiated energy is immediately absorbed by the capsule. However a substantial portion of the outward-radiated energy is reflected from the outer hohlraum walls rather than lost, as is a substantial proportion of energy striking the hohlraum floor, so about two-thirds, 1.46 MJ will ultimately be absorbed by the capsule, over 7× greater than NIF: only 5.9× greater than NIF is required.

As the imploding fuel reaches its minimum diameter, the ignition pellets incoming from the direction of the long arrow strike it as a compressed mass. The purpose of the central 'chimney' is to minimize the thermal energy and plasma the IG pellets encounter before hitting the compressed fuel.

2.11 Reaction chamber

Fusion takes place within a chamber containing a liquid lithium waterfall broadly as described in [16, pp 14-38]. However the chamber, illustrated in Figure 4, has the following significant differences:

- The central void is just 50 cm in diameter.

- The waterfall comprises closely spaced vertical jets ~1 cm diameter each. The central jets are pulsed so that a central void occurs at the required moment.

- The net radial thickness of liquid lithium in the waterfall is 100 cm (plus 50 cm outside the waterfall chamber in the recirculation flow).

- Heat exchanger to extract energy, and electromagnetic pump to circulate the lithium, are situated at the base of the chamber.

- Lithium waterfall enters the chamber at ~500°C, the maximum temperature compatible with prolonged contact with stainless steel.

- For each detonation a sacrificial projectile, comprising a hollow tube with the hohlraum containing the fuel capsule at its front end and the rear end open, is fired to the centre of the waterfall via a pipe. The primary purpose of the projectile is to ensure that pellets travel through high vacuum all the way to the hohlraum. A useful secondary purpose is to protect the end of the pipe. While the chamber itself has indefinite working life, the pipe is relatively inexpensive and can be replaced at regular intervals.

Total release of energy from each detonation is 500 MJ, in the form of 400 MJ from fusion, of which 320 MJ is fast neutrons and 80 MJ α-particles, plus 100 MJ from fission induced in the lithium. All but the 80 MJ α-particles has no explosive effect, but is directly dumped thermally into the lithium. One cc of liquid lithium 25 cm from the detonation absorbs 400 J of neutron energy plus 100 J from induced fission, raising its temperature from 500°C to 780°C, still well short of its boiling point.

The central part of the chamber is shown at larger scale in Figure 5. The projectile is made of lithium, the delivery pipe of a refractory material such as graphite. The projectile walls are thick towards the rear to scatter neutrons, but thin towards the front to minimize mass in the vicinity of the explosion, hence momentum generated. The hohlraum containing the fuel capsule forms the projectile front end. The projectile is fired in along the pipe at ~100 m/s. It is shown just before detonation, when the ignition and hohlraum-heating pellets have passed through the pipe and the projectile interior and are about to reach the hohlraum.

The central part of the chamber contains a fairly good vacuum initially, lithium vapor at ~$10^{-2.5}$ torr[16, Figure 8]. This vapor cannot leak back past the projectile in time to obstruct the passage of the pellets through the much better vacuum maintained in the pipe and projectile interior.

Figure 4   Detonation chamber

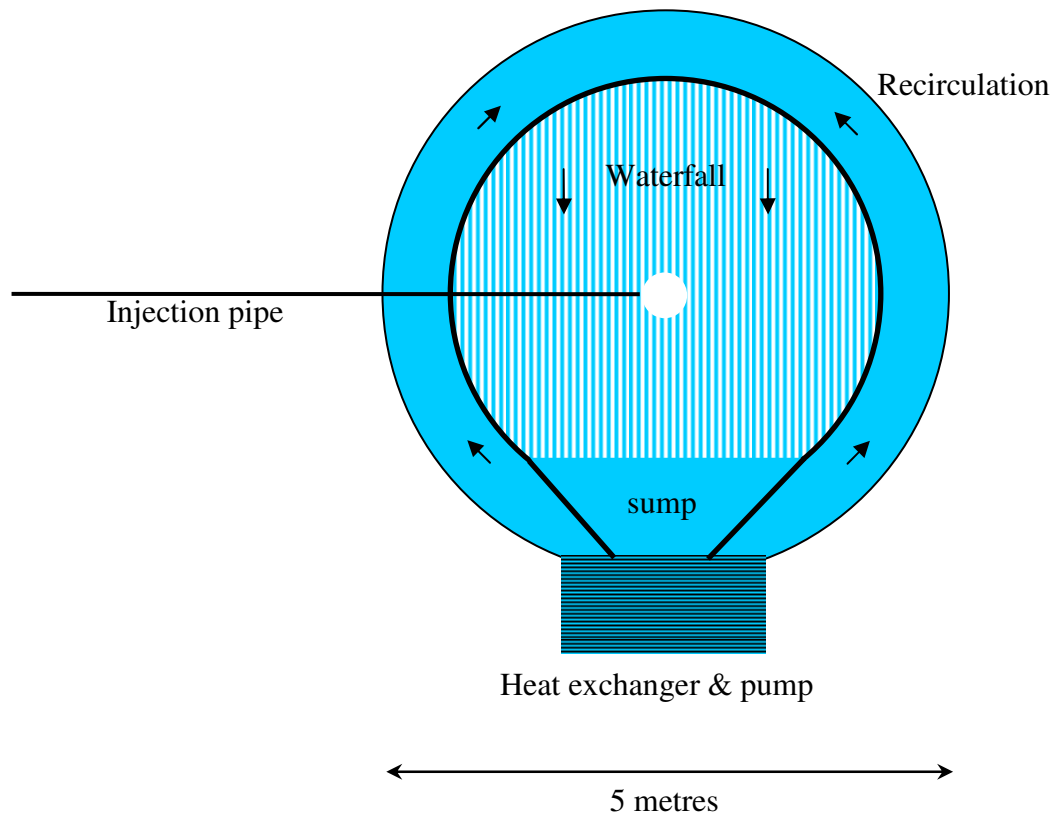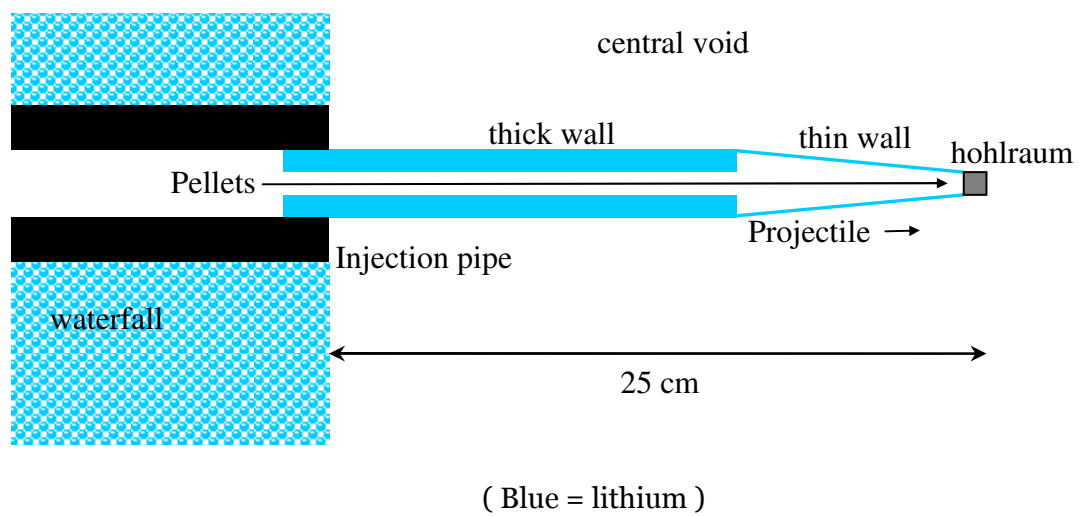Recirculation

Waterfall

Injection pipe

sump

Heat exchanger & pump

5 metres

Figure 5   Chamber centre with projectile

central void

thick wall

thin wall

hohlraum

Pellets

Projectile →

Injection pipe

waterfall

25 cm

(Blue = lithium)

Neutrons from the central detonation travelling towards the pipe end pass through ~10 cm slant length of projectile wall en route. While this absorbs only ~10% of their energy, they are also scattered. As there is vacuum in all other directions, this scattering reduces the neutron energy striking the pipe end by at least an order of magnitude. One cc of the pipe end absorbs at most 40 J per detonation = 200W, which is thermally radiated from the pipe outer surface. The pipe end is additionally cooled by liquid lithium from the rear part of the now-melted projectile flowing out after the detonation.

Energetic α-particles vaporize the hohlraum to plasma. However because this constitutes a small mass ~1 g, although the energy absorbed is 80 MJ, the associated momentum pulse is only ~400 kg.m/s, comparable to the detonation of 200g of TNT. The presence of the projectile material as a barrier ensures that none of this plasma impacts the pipe.

A pulsed pumping rate of ~20 m^3 per detonation provides 1 m net lithium waterfall thickness, giving a stainless steel chamber indefinite working life[16]. Additional liquid lithium circulates outside the chamber wall, to ensure that almost all neutrons produced are absorbed. Neutrons from the DT reaction are absorbed by ^{6}Li to produce tritium; or by ^{7}Li to produce both a tritium and a lower energy neutron, which can then breed a further tritium from ^{6}Li. Natural lithium comprises a mixture of these isotopes, 7.5% ^{6}Li to 92.5% ^{7}Li: this ratio can easily be altered by fractional distillation. Thus it is straightforward to fine-tune the system so that exactly 100% of the tritium required for continued operation is produced.

Part of the lithium flow is circulated through a divertor to recover the contaminants introduced. After heating the lithium to a gas, carbon, glass and metal are recovered as particles of soot, sand, and dust. As the lithium subsequently cools to liquid in near-vacuum, hydrogen gas (protium, deuterium and tritium) and helium (from the α-particles produced) is pumped away. The sacrificial projectiles, which are simple in form and can be made to quite crude tolerances, are made cheaply and continuously by tapping some of the molten lithium into moulds.

Optionally, the arrangement of Figure 4 can be placed within an outer enclosure comprising a wall of moderator such as graphite beyond which is a double-walled tank of ^{6}Li. The neutron capture cross-section of ^{6}Li increases vastly as neutron speed decreases[4, p45]. Circulated separately to recover tritium and helium, this outer lithium reservoir ensures that virtually no neutrons escape the system.

Thermal energy available after capsule detonation is 400 MJ from fusion + 100 MJ from induced fission in the lithium + 4 MJ pellet kinetic energy = 504 MJ. The liquid lithium is circulated through a heat exchanger by electromagnetic pump to boil water. This generates 210 MJ of electricity @42% efficiency, of which 10 MJ is diverted to the accelerator to provide the next pellet pulse. Net electricity output is 200 MJ. 5 detonations per second drive a 1-GW power station.

2.12 Cost

A 2.5 km long building is required to house the system, providing an environment of dry air at constant temperature. A single-storey steel frame building on cheap land costs up to $400/m² footprint[17] including foundations and labor. On this basis a building consisting of a 5m wide corridor would cost $2,000/m. However the building must run straight and level for its entire length. Ground preparation cost may therefore be higher than normal. A double-track railroad on cheap land without geophysical complications costs ~$5,000/m[18]. Total cost of the accelerator building, including foundations and construction, is therefore put at ~$6,000/m = **$15 million**.

(Even if the entire system must be placed in a tunnel, this adds only ~$40,000/metre to the cost, a further **$100 million**[18].)

The dominant cost element of the accelerator is the RF power MOSFETs: from section 2.7, **$100 million**. The cost of cooling and of power supply/conditioning upstream of the MOSFETs will be relatively modest. Volumetric cost of raw materials for the accelerator tubes is ~$60/litre for virgin grade Teflon and copper, less for other materials such as stainless steel. Allowing for installation, control systems and auxiliary equipment such as the fiber feed system and trajectory adjustment stations, total accelerator system cost is put at ~**$200 million** if on the surface or ~**$300 million** if in a tunnel.

The remaining part of the power station, comprising steam turbines, generators, cooling towers, etc., is very similar to coal-fired plant. The compact lithium chamber and its associated equipment are assumed to replace a furnace and coal handling equipment of comparable or greater cost. Capital cost of a 1 GW coal-burning power station is ~**$3 billion**[19, Table 1]: the accelerator is a relatively small ~10% addition to this.

Consumable cost will be negligible, compared to ~$200 million/annum per GW for a coal-fired plant at typical US coal price ~$65/tonne[20]. Glass fiber, deuterium and lithium are required in very modest quantities. The hohlraum

assemblies containing hemispherical fuel capsules are much easier to manufacture than NIF-type full spheres. Neither hohlraum nor fuel capsule need to be made of layers of differently doped materials, because maximally efficient hohlraum reflection and capsule absorption of X-ray energy (desired for NIF because laser energy is expensive to provide) and precise pulse shape tailoring (needed in NIF to provide the central ignition peak) are not necessary.

If the cost of manufacturing the fuel-capsule-plus-hohlraum assemblies is problematic, scaling laws make it relatively cheap to use fewer, larger detonations. For example to quadruple the energy release per pulse, from 500 MJ to 2 GJ, requires increasing the diameter of the lithium chamber by only 0.5 m. The fusion gain obtained increases with larger fuel mass, so the compression energy which must be supplied also increases less than linearly with output.

A particularly exciting prospect is that in many locations, existing coal-fired plants could be retrofitted for fusion. This is realistic because:

- The neutron capture cross-section of ^{6}Li increases vastly as neutron speed decreases[4, p45], so neutron flux escaping the system can be made negligible.

- It is possible to remove virtually all hydrogen (of all isotopes) from liquid metal, to ~1 part per million. This is done, for example, to produce maraging steel. So although tritium is produced and extracted, the tritium inventory at any given instant can be very modest, a few grams. There are no other radioactives present which could escape.

Such an ultra-clean fusion system, retrofitted to an existing coal-fired station, could recoup its cost within two years.

3. DEVELOPMENT PATH

I wish to remain involved in development after an entity with suitable resources has purchased the IP, and I will have significant further input at this stage.

An outline development route is:

1. A first demonstration that a metal-coated glass fiber with a high length/width ratio can be charged to high voltage, fired through an AC accelerator, and actively steered as described. This can be done very cheaply using a laboratory-scale accelerator ~ 1 metre length to fire fibers to 100 km/s, the speed used to test meteor shields for interplanetary spacecraft.

2. A second demonstration, using the same system, that such a fiber contracts upon in-flight discharge by electron gun.

3. A third demonstration, using the same system, that a series of such fibers fired at differential speed can be made to converge in flight.

4. A fourth demonstration of actual (non-ignition) fusion can use a 50 nm diameter S-2 glass fiber, the smallest so far demonstrated to be makeable[9], with charge/mass ratio 8× that of the IG fibers in section 2. This fiber is accelerated to 4,000 km/s in an accelerator ~50 m long.

   Fired into a target comprising a thin layer of frozen deuterium on a backplane of gold, the impact of a single fiber will produce temperature ~10 keV , hence easily detectable fusion neutrons.

   This is a significant milestone (unlike firing individual nuclei into a target to fuse) because with the capacity to accelerate and control macroscopic objects proved, progress to ignition and power production is merely a matter of scaling up.

There will be very high confidence from this point onward that ignition can be achieved, because if necessary several times the ignition energy and concentration derived in Section 2 could be provided at acceptable cost. Ignition then follows from basic conservation of momentum and energy considerations, however pathological the plasma behavior.

APPENDIX 1 : PELLET CHOICE

Maximum negative charge which can be placed on a macroscopic object in vacuo is limited by field effect electron emission. The pellets are therefore positively charged. Maximum positive charge is limited by burst-apart due to self-repulsion, and field evaporation. These are really two sides of the same coin: unless long periods at high temperatures are involved, burst-apart is the limiting factor.

Spherical pellet

If the pellet is a sphere, charge will distribute itself evenly over the surface. The burst-apart force calculation is then mathematically identical to the well known case of the self-gravity of a thin spherical shell. A point mass **m** at a distance **R** from the centre of a spherical shell of mass **M** experiences a gravitational pull of **GmM/R²** in the space outside the shell, and zero everywhere inside it. An average particle of the shell itself thus experiences **GmM/2R²**. The mass per unit area is **M/4πR²**, giving an inward surface pressure of **GM²/8πR⁴**. The corresponding outward pressure on a spherical shell carrying charge **Q** is **kQ²/8πR⁴**, where **k = 1/4πε₀**. This must not exceed the safely usable strength **σ** of the material, so maximum charge permissible is **5.3x10⁻⁵ R²√σ**. The mass of the sphere is **(4/3)πR³ρ**, so the maximum charge/mass ratio is

$$Q/M = \frac{1.26 \times 10^{-5}\sqrt{\sigma}}{R\rho} \qquad \textbf{[Eqn. 5]}$$

Small diameter pellets can thus be given higher charge/mass ratio than large diameter ones.

Fiber pellet

The fiber case cannot be solved analytically, because longitudinal tension does not tend to a limit as length tends to infinity, although it increases very slowly. (Analytically, the sum of the harmonic series 1 + ½ + 1/3+ 1/4... is involved.)

The corresponding calculation must therefore be done by a finite element method. I have written a simple computer program which allows charge to move longitudinally to approximate equilibrium before calculating the tension. The program is available free on request: approximate verification by hand calculation is also possible, treating the fiber as uniformly spaced a line of point charges.

As with spheres, smaller diameter fibers can be given proportionately higher charge/mass ratio than large diameter ones. Charge per unit length is nearly constant except very close to the ends. In order that a fiber can be accelerated while remaining straight, hence not vibrate when the accelerating field is switched on or off, charge/mass ratio should be the same everywhere along its length. This can be

achieved by tapering the fibers, or by applying a metal coating of varying thickness and/or density.

Pellet choices are compared in Table 3. Tensile strength safety factor 1.5 is assumed in each case. For the fiber, longitudinal stress is an order of magnitude greater than radial. The fiber is assumed initially cooled to -200°C, which significantly increases its strength.

TABLE 3   Pellet comparison (mass 50 picograms)

material	strength GPa	density g/cc	diam μm	length μm	Charge pC
Diamond UNCD	3.0	3.5	3	-	5.3
Maraging steel	2.4 *yield*	8.1	2.25	-	2.7
Al-Li Weldalite alloy	0.69 *yield*	2.7	3.25	-	3.0
S-2 glass fiber[8]	8.3	2.5	0.1	2500	88

Metal microspheres can readily be made by spraying droplets which cool as they fall, the method originally used to make ball bearings. Weldalite and maraging steel are suitable choices as they reach their exceptional strength without cold working. However even including diamond in the options, glass fiber performs better than any approximately spherical pellet of comparable mass, for reasons both of geometry - its charge being spaced further apart - and high tensile strength. Glass fiber is cheap, and it is easy to feed continuous fiber chopped by laser as it enters the accelerator. S-2 glass has excellent strength, increasing from 5 GPa in a room environment to 8.3–11.6 GPa if initially cooled to cryogenic temperature. In this paper maximum tensile load 5.53 GPa is assumed, i.e. a safety factor of 1.5 w.r.t. the lower cryogenic measured strength.

 (Carbon fiber is not a preferred choice due to lack of radial strength and because it can be made only in a limited range of diameters ~5–10 μm. In principle exotic forms of carbon are much stronger then the above options and could carry higher charge without burst-apart, but are at present too expensive to be a viable choice.)

APPENDIX 2 : SCALING LAWS FOR FAST IGNITION

With ρ in units of 100 g/cc, ignition thresholds for energy, work rate, intensity, and radius scale as[4, p411-412]:

$E \sim \rho^{-1.85}$

$W \sim \rho^{-1}$

$I \sim \rho^{0.95}$

For a cylindrical bullet impact we can derive thresholds for impact duration **T**, area **A**, radius **R**, and kinetic energy delivered per unit area **S**:

$T \sim \rho^{-0.85}$

$A \sim \rho^{-1.95}$

$R \sim \rho^{-0.98}$

$S \sim \rho^{0.1}$

Note that **S** is almost constant regardless of fuel density. This turns out to be the most demanding threshold for the pellet impact method. A bullet formed from pellets can compress axially to a thin disk: because compression is uniform with small relative speed between neighbors, it is adiabatic and not limited by shock heating. So very high volumetric density can be achieved, to deliver energy at high work rate and intensity. However as axial compression occurs, bullet diameter increases, limiting the energy per unit area.

REFERENCES

1. On The Attainability Of Fusion Temperatures Under High Densities By Impact Shock Waves Of Small Solid Particles Accelerated To Hypervelocities
   F. Winterberg, *Z. f. Naturforsch.* 19a, 231 (1964)

2. The Ignition Of Dense DT Fuel By Injected Triggers
   A. Caruso, V.A. Pais, Nuclear Fusion, vol. 36 p745 (1996)
   http://iopscience.iop.org/0029-5515/36/6/I06

3. Hypervelocity microparticle characterization, G.C. Idzorek (1996)
   http://www.osti.gov/bridge/servlets/purl/397131-QIEjdF/webviewable/397131.pdf

4. The Physics Of Inertial Fusion, S. Atzeni & J. Meyer-Ter-Vehn, OUP (2004)

5. Tutorial on the Physics of Inertial Confinement Fusion, R. Betti (2011), 3rd Meeting of the NAS Panel on Inertial Fusion Energy Systems http://fire.pppl.gov/IFE_NAS3_ICF_tutorial_Betti.pdf

6. Fast Ignition Studies at Sandia National Laboratories, R Campbell et al. (2005)
   http://www.sandia.gov/pulsedpower/prog_cap/pub_papers/055784c.pdf

7. Cryogenic thermonuclear fuel implosions on the National Ignition Facility
   S. H. Glenzer et al., Physics of Plasmas, vol. 19 issue 5 (2012)
   http://www.psfc.mit.edu/icf/Home%20Page/Papers/Glenzer_PoP-2012.pdf

8. High Strength Glass Fibers, D. Hartman et al., AGY Ltd. (1996)
   http://www.agy.com/wp-content/uploads/2014/03/High_Strength_Glass_Fibers-Technical.pdf

9. Mazur Group
   http://mazur.harvard.edu/research/detailspage.php?rowid=11

10. High Gradient Operation of 8-GeV C-Band Accelerator in SACLA, T. Inagaki et al. Proceedings of LINAC2012 (2012) https://accelconf.web.cern.ch/accelconf/LINAC2012/papers/mopb005.pdf

11. High Gradient Performance of RF Gun, T. Taniuchi, International Workshop on Breakdown Science and High Gradient Technology (2012)
    http://indico.cern.ch/event/165513/material/slides/1?contribId=40

12. Electric Field Limits For Vacuum Breakdown, S. Humphries
    http://fieldp.com/myblog/2011/electric-field-limits-vacuum-breakdown/
    based on High Voltage Breakdown in the Electron Gun of Linear Microwave Tubes,
    A.J. Durand and A.M. Shroff *in* High Voltage Vacuum Insulation, R.V. Latham (ed.), Academic Press, London (1995)

13. http://www.farnell.com/datasheets/66935.pdf

14. http://www.farnell.com

15. http://www.ti.com/product/ads4249/description

16. Reactor Concepts for Laser Fusion, W Meier & J Maniscalco (1977)
    http://www.osti.gov/bridge/servlets/purl/5232953-TPTXcg/5232953.pdf

17. http://www.buildingsguide.com/faq/what-average-commercial-building-cost-square-foot

18. Calculating Rail Construction Costs In Light Of The Eddington Report (2008)
    http://melbpt.wordpress.com/2008/04/26/calculating-rail-line-construction-costs-in-light-of-the-eddington-report/

19. Updated Capital Cost Estimates for Utility Scale Electricity Generating Plants (2013), U.S. Energy Information Administration
    http://www.eia.gov/forecasts/capitalcost/

20. http://www.infomine.com/investment/metal-prices/coal/5-year/